Supplement of The Cryosphere, 15, 4853–4871, 2021
https://doi.org/10.5194/tc-15-4853-2021-supplement

The Cryosphere Open Access EGU

Supplement of

Impact of lateral groundwater flow on hydrothermal conditions of the active layer in a high-Arctic hillslope setting

Alexandra Hamm and Andrew Frampton

Correspondence to: Alexandra Hamm (alexandra.hamm@natgeo.su.se)

Supplementary method I: Pan-Arctic slope categorization

To calculate the slopes represented in Figure 1 in the main text, we utilized the ArcticDEM 10 m resolution product (Porter et al., 2018). The extent is limited to areas with continuous permafrost according to Brown et al. (2002). In order to subset the information into smaller areas, different administrative areas of countries within the extent of the ArcticDEM were chosen. These administrative areas include Alaska (US), Yukon (CA), Northwest Territories (CA), Nunavut (CA), Quebec (CA), Greenland (DK), Svalbard (NO), Northwestern Federal District (RU), Ural (RU), Siberia (RU) and Far Eastern Federal District (RU). In each region, ArcticDEM tiles have been downloaded within the area of continuous permafrost. All tiles are masked to the area of continuous permafrost to avoid artifacts over the sea surface. Slopes have been calculated and reclassified using GDAL (GDAL/OGR contributors, 2021). The classification is based on the categories described in the main text for the area of Adventdalen. The exact values represented in Figure 1 in the main text can be found in Table S1 and provide a good first estimate of landscape inclinations in reference to this paper.

Region	**<5°**	**5-15°**	**15-25°**	**>25°**
Alaska	71.60	17.19	5.63	5.58
Yukon	40.34	27.21	13.84	18.61
Northwest Territories	75.93	14.94	3.80	5.33
Quebec	67.00	24.21	4.47	4.33
Nunavut	71.94	18.32	4.99	4.74
Greenland	41.89	30.44	13.03	14.64
Svalbard	58.27	21.16	8.05	12.52
Northwest	74.47	17.31	4.63	3.60
Ural	84.36	12.45	2.16	1.03
Siberia	77.11	19.40	2.52	0.97
Far East	59.99	22.82	8.70	8.49
Average	**65.71**	**20.50**	**6.53**	**7.26**

Table S1: Calculated percentages of each slope class for each region considered for the evaluation.

Supplementary figures

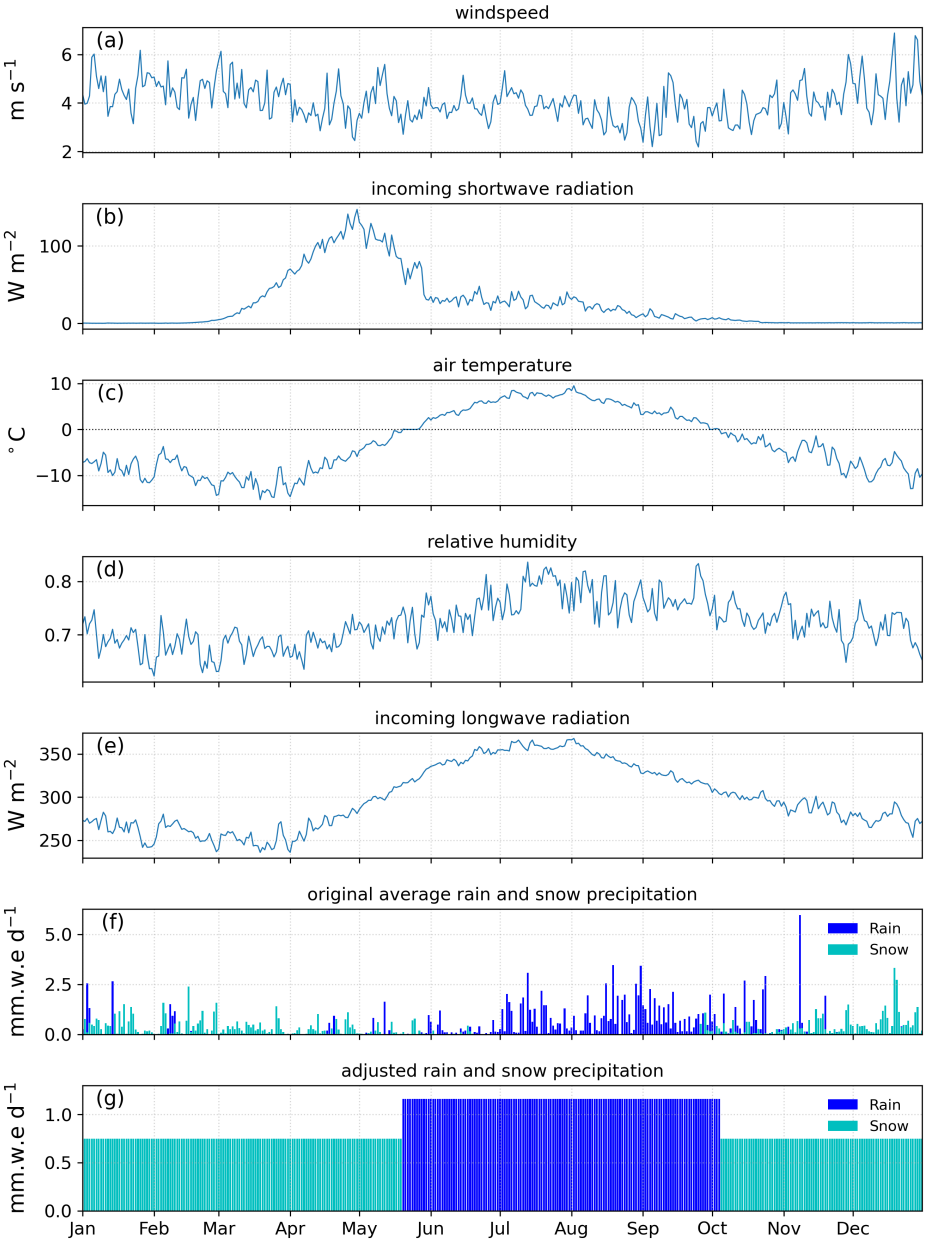

Figure S1: Daily values of the forcing dataset averaged over the 2013–2019 period (DOY-average). Precipitation in **g** was adjusted by defining a rain period (air temperature $> 0\,°$) and a snow period (air temperature $\leq 0\,°$) and equally distributing the by for each day in the respective period.

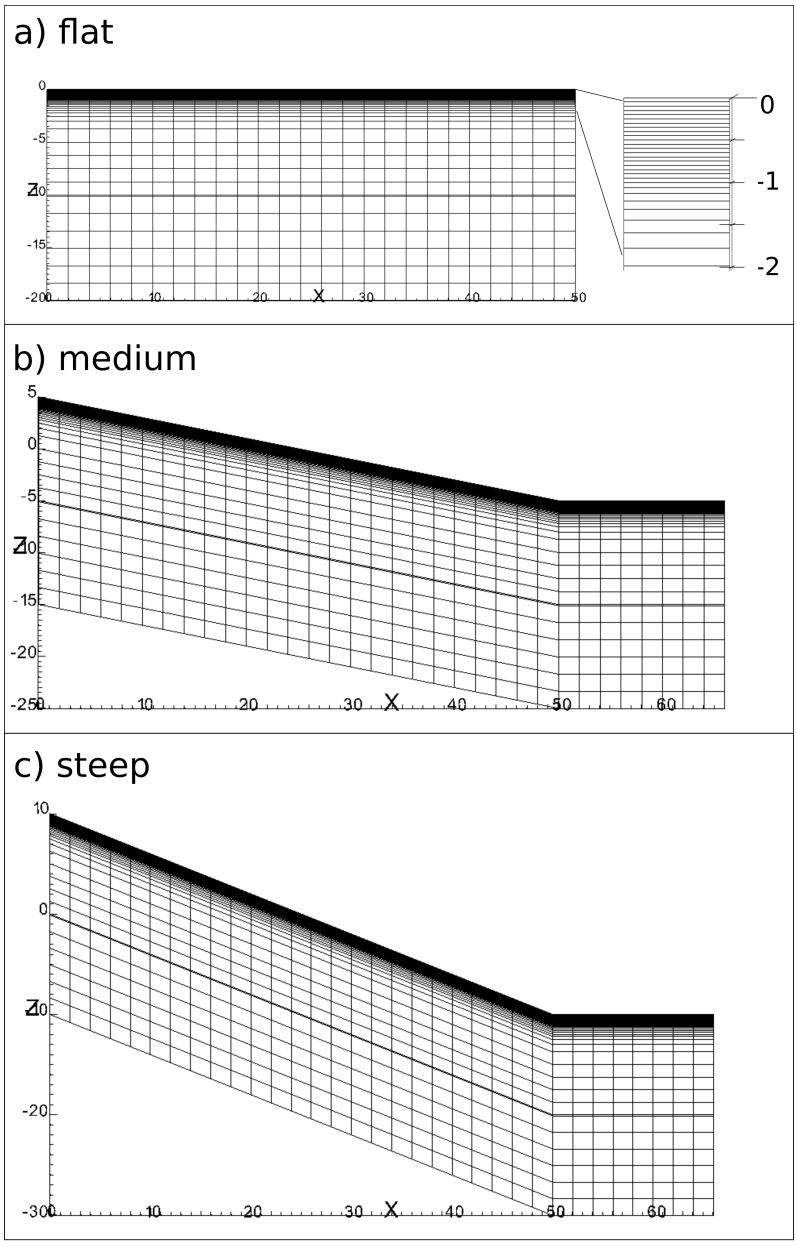

Figure S2: Representation of the meshes used in this study. **a** represents the mesh for the flat case, **b** represents the medium and **c** the steep mesh. **a** also shows a detailed representation of the upper two meters of each column of each subsurface mesh. All meshes extend 20 m in z-direction and 1 m in y-direction (not visible). The flat mesh extends 50 m in x-direction, while the slopes extend 66 m in x-direction to avoid edge-effects on the lower end of the slope. The additional 16 m represent a conceptual valley bottom until the no-flow boundary condition on the right side, which represents a symmetry boundary condition.

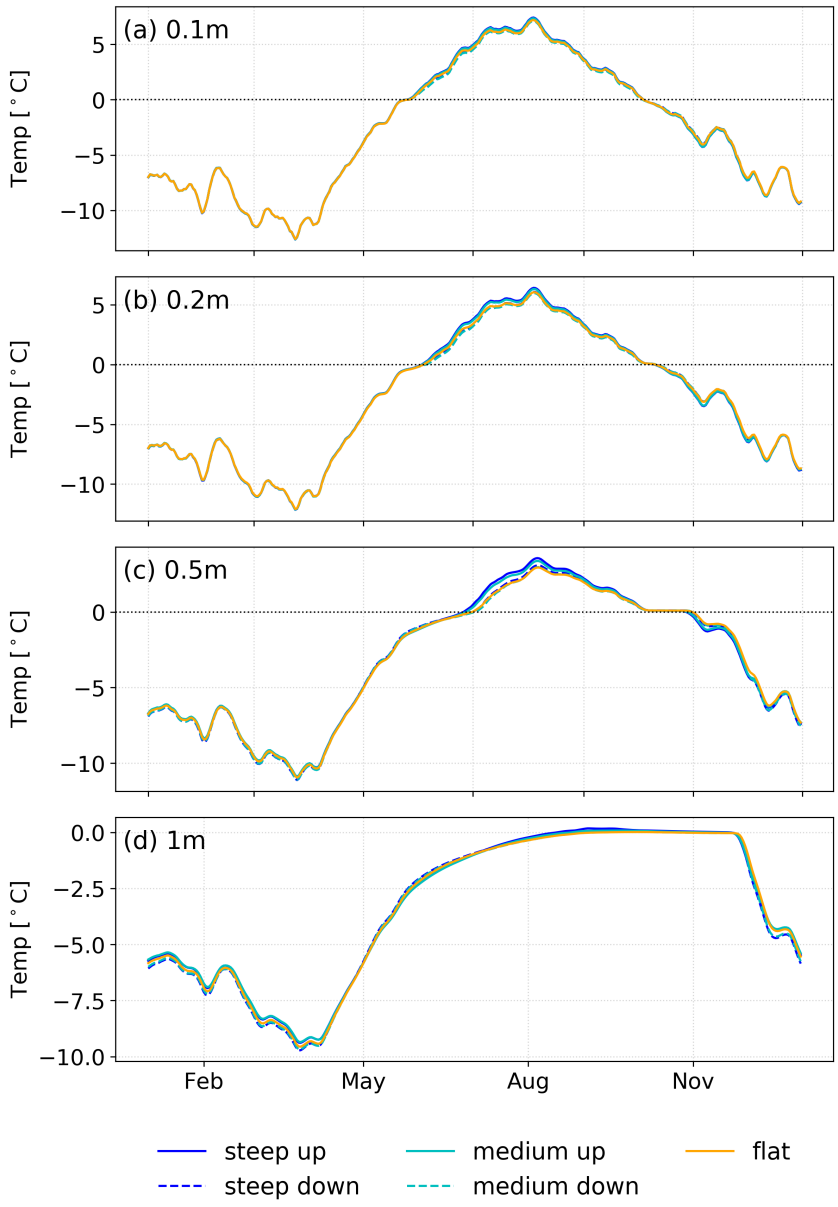

Figure S3: Time series of daily temperature (7-day moving average) in the four different depths used for deriving temperature differences in Fig. 3 in the main text. Note that the vertical axis varies between each plot. The horizontal dotted line in plots **a**,**b**, and **c** indicates 0 °C . The three different cases are indicated by blue (steep), cyan (medium) and yellow (flat) colors.

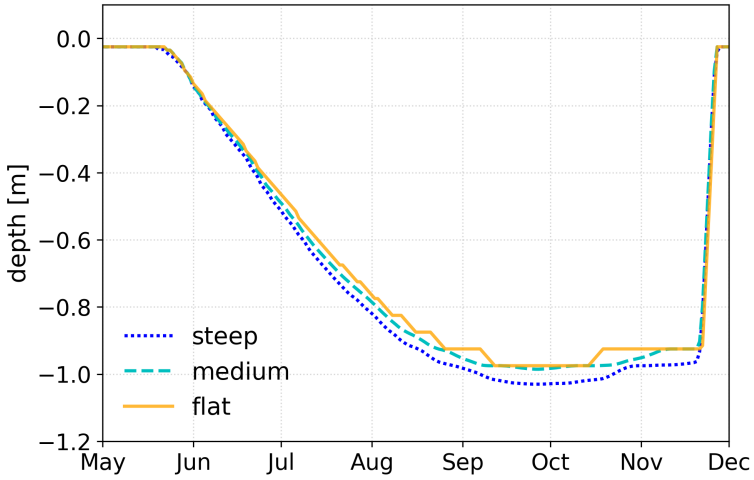

Figure S4: Representation of thaw depth compared between the steep (blue), medium (cyan) and flat case (yellow) as daily, spatially averaged thaw depth (averaged over a 5-day window) from May to December in the last year of the simulation. Note that thaw depth is defined as cells within the model domain that exceed 0 °C.

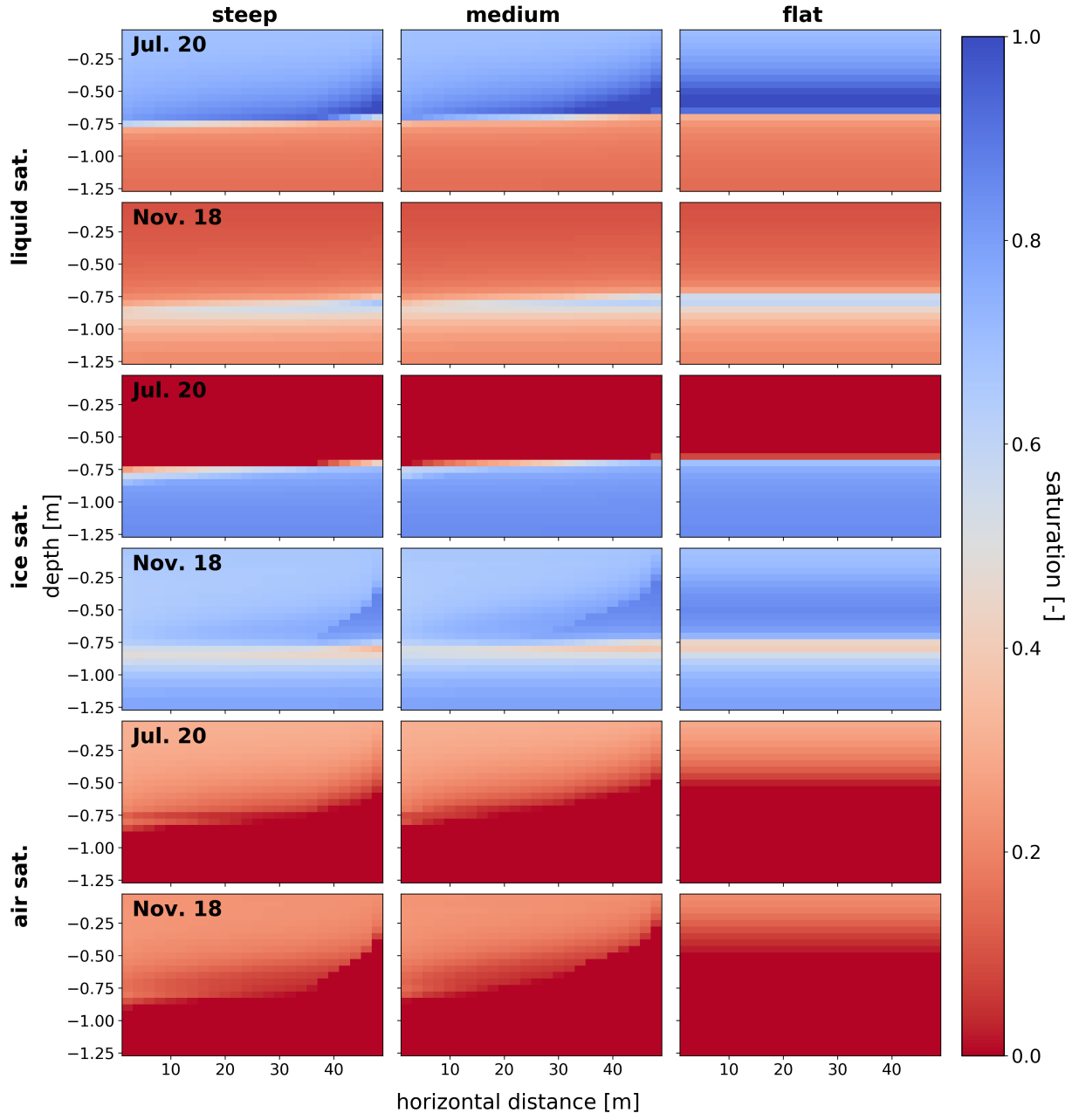

Figure S5: Representation of liquid- (rows 1 and 2), ice- (rows 3 and 4), and gas saturation (rows 5 and 6) on summer day (July 20) and a winter day (November 18) throughout the transect (representation of the upper 1.2 m of the model domain across the 50 m slope transect). Red colors represent low saturation, blue colors high saturation.

Figure S6: Surface snow depth during the last year of the simulation representative for each column of the model domain of all three steepness cases (flat, medium, steep slope).

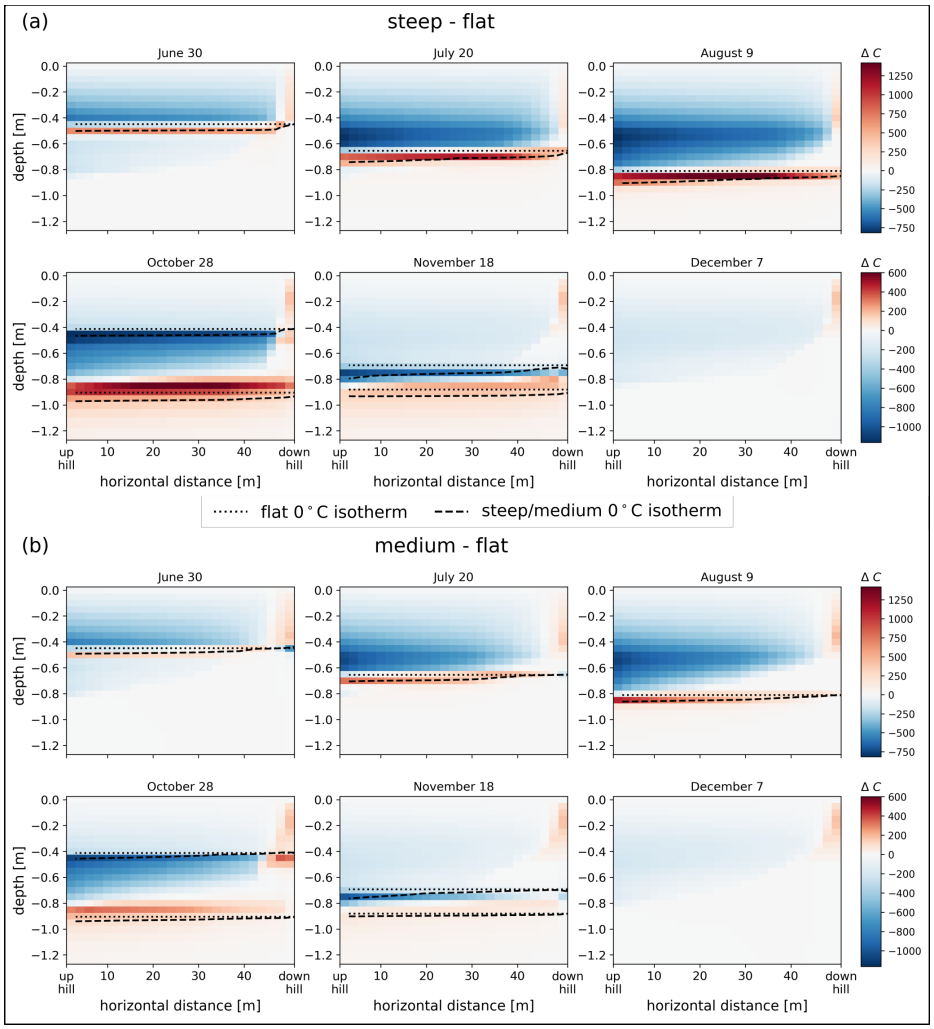

Figure S7: Differences in heat capacity (C) between **a** the steep and the flat case and **b** the medium and flat case at six selected dates, which correspond to the same dates as in Fig. 4 in the main text. Red colors indicate higher heat capacity in the hillslope cases than in the flat case, blue colors indicate lower heat capacity (note the color scale differs between summer and winter comparisons). The black dotted line indicates the 0 °C isotherm(s) in the corresponding hillslope case at the respective dates. The figure only shows the upper 1.2 m of the entire simulation domain extends to 20 m below the surface.

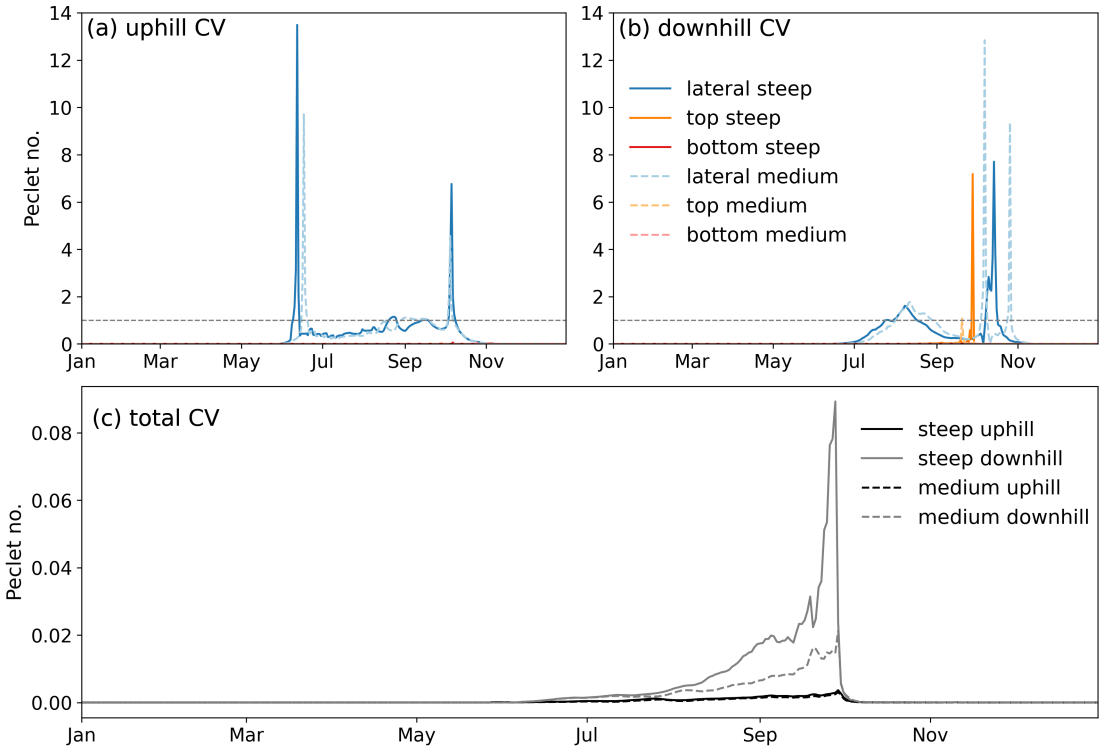

Figure S8: Daily ratio between advective and diffusive energy flux on each of the faces of the **a** uphill CV, **b** downhill CV and **c** the entire CV. Solid lines represent values for the steep case, dashed lines represent the medium case, while colors indicate the different faces of the CV. Dashed horizontal lines in **a** and **b** indicate the value of 1, where the advective energy flux becomes more pronounced than the diffusive energy flux. Note that there is no such line in **c**, as the Péclet number over the total CV is very small.

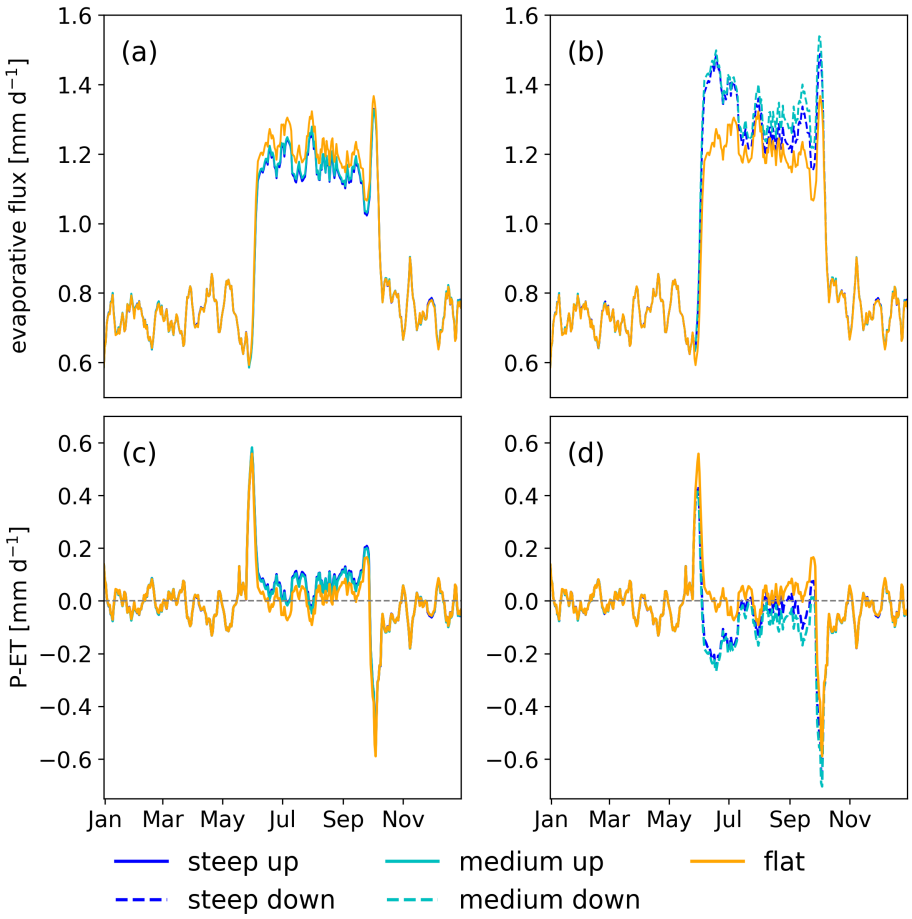

Figure S9: Evaporative flux (**a** and **b**) and net infiltration (precipitation-evaporation; **c**, **d**) at the surface on the uphill (solid lines; **a** and **c**) location and the downhill (dashed lines; **b** and **d**) location. Daily values are averaged over a 7-day window. Blue, cyan and yellow represent the steep, medium and flat case, respectively.

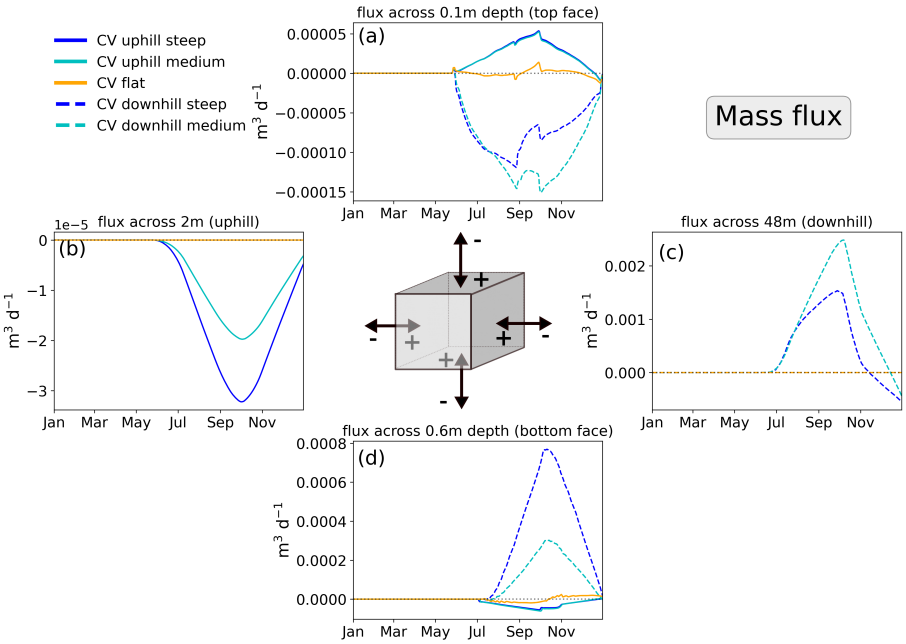

Figure S10: Daily values of mass flux through the faces of the control volume (CV; 90-day moving average) at the uphill (solid) and downhill (dashed) CV locations. Colors represent the steep (blue), medium (cyan) and flat (yellow) case, respectively. The sign convention adopted is positive values represent heat entering the CV and negative values leaving the CV. Due to the definition of the CV boundaries, lateral fluxes only occur on the right face for CV up and on the left side for CV down.

Supplementary tables

Table S2: Maximum temperature difference between uphill and downhill observation sides (ΔT_E) at several depths within the active layer for each hillslope case; positive values indicate warmer temperatures occur uphill (steep or medium) compared to downhill.

ΔT_E	0.1 m	0.2 m	0.4 m	1 m
steep	0.49	0.62	0.74	0.46
medium	0.46	0.61	0.69	0.42

Table S3: Maximum temperature difference between various hillslope inclination cases (ΔT_I) at several depths within the active layer; positive values indicate warmer temperatures occur in the sloped (steep or medium) cases compared to the flat case.

ΔT_I	**uphill**				**downhill**			
	0.1 m	0.2 m	0.5 m	1 m	0.1 m	0.2 m	0.5 m	1 m
steep-flat	0.27	0.45	0.80	-0.42	-0.21	-0.21	-0.46	-0.49
medium-flat	-0.21	0.34	0.56	-0.34	-0.28	-0.31	-0.41	-0.41

Table S4: Maximum temperature difference between various hillslope inclination cases (ΔT_I) at several depths within the active layer; positive values indicate warmer temperatures occur in the sloped (steep or medium) cases compared to the flat case.

		June 30	July 20	August 9	October 28	November 17	December 7
S1R1	steep	0.73	1.72	2.02	-0.70	-0.85	-5.14
	medium	0.65	1.60	1.90	-0.68	-0.82	-5.10
	flat	0.56	1.47	1.79	-0.64	-0.78	-5.06
S0R0	steep	2.09	3.41	3.84	-0.84	-1.09	-4.96
	medium	1.98	3.34	3.77	-0.81	-1.05	-4.86
	flat	1.96	3.29	3.73	-0.79	-1.03	-4.81
S2R2	steep	0.15	1.08	1.34	-0.70	-1.13	-5.85
	medium	0.05	0.94	1.22	-0.69	-1.17	-5.89
	flat	0.01	0.89	1.17	-0.69	-1.21	-5.92

References

Brown, J., Heginbottom, J., Ferrians, O., and Melnikov, E.: Circum-Arctic Map of Permafrost and Ground-Ice Conditions, Version 2, https://doi.org/10.7265/SKBG-KF16, URL https://nsidc.org/data/GGD318/versions/2, type: dataset, 2002.

GDAL/OGR contributors: GDAL/OGR Geospatial Data Abstraction software Library, Open Source Geospatial Foundation, URL https://gdal.org, 2021.

Porter, C., Morin, P., Howat, I., Noh, M.-J., Bates, B., Peterman, K., Keesey, S., Schlenk, M., Gardiner, J., Tomko, K., Willis, M., Kelleher, C., Cloutier, M., Husby, E., Foga, S., Nakamura, H., Platson, M., Wethington, M., Williamson, C., Bauer, G., Enos, J., Arnold, G., Kramer, W., Becker, P., Doshi, A., D'Souza, C., Cummens, P., Laurier, F., and Bojesen, M.: ArcticDEM, https://doi.org/10.7910/dvn/ohhukh, URL https://dataverse.harvard.edu/citation?persistentId=doi:10.7910/DVN/OHHUKH, type: dataset, 2018.